A new hybrid method for the fast computation of airgap flux and magnetic forces in IPMSM

Emile Devillers, Michel Hecquet
L2EP, University of Lille, Centrale Lille
CS 20048
Villeneuve d'Asq, France
Email: emile.devillers@phd.ec-lille.fr

Emile Devillers, Jean Le Besnerais
EOMYS ENGINEERING
121, rue de Chanzy
Lille-Hellemmes, France
Email: jean.lebesnerais@eomys.com

***Abstract*— In this paper, a new hybrid method is developed for the fast and accurate computation of air gap flux density in the open-circuit Interior Permanent Magnet Synchronous Machines (IPMSM). The rotor magnetomotive force is estimated using a single non-linear FEA simulation. Then, rotor motion and stator slotting effect are included without loss of calculation performance using the semi-analytical subdomain method initially developed for Surface Permanent Magnet Machines. This hybrid method calculates the time and spatial distribution of radial and tangential airgap flux in a few seconds. It can be used to quickly estimate electromagnetic quantities (cogging torque, back emf) as well as magnetic forces for the electromagnetic and vibroacoustic design optimization of electric motors. The method is applied to the vibroacoustic analysis of the IPM machine of the Toyota Prius 2004 at open-circuit state and variable speed. Results show that the maximum sound power level occurs when the air gap magnetic pressure harmonics excite the breathing mode of the stator structure.**

Keywords*—*Interior permanent magnet machine; Flux density computation; Magnetic noise and vibrations ; Subdomain method ; Hybrid approach.

I. INTRODUCTION

In electrical machines, the study of noise and vibrations due to magnetic forces requires an accurate knowledge of the time and spatial distribution of the air gap magnetic field in radial and tangential directions. Indeed, a very small magnitude harmonic in the magnetic forces can induce large noise and vibrations if a resonance with a structural mode of the machine is met. One can show that the lowest force wavenumbers give the largest structural deflections, but as the magnetic force is a quadratic function of the flux density, this means that some high flux density wavenumbers can be involved in noise generation, so the airgap distribution of the flux must be evaluated accurately. Moreover, the tangential field can be significant due to larger airgap compared to induction machines, and it can potentially affect radial magnetic force harmonics [1].

In Interior Permanent Magnet (IPM) machines, the harmonic content of the magnetic field strongly depends on the rotor topology, including IPM position and rotor bridges. The simplest way to minimize cogging torque, noise and vibrations level and obtain the best electromechanical performances is to perform a global optimization during the machine design. Such optimization is only feasible thanks to a fast computation of the air gap magnetic field and resulting magnetic forces.

The Finite Element Analysis (FEA) is currently the most reliable solution to obtain the magnetic field distribution of IPM machines. This numerical method accounts for any rotor topologies, saturated rotor bridges, stator slotting effect and local stator teeth saturation. However, it is too much time-consuming when considering a fine discretization to observe high time and space harmonics of magnetic field, and a fine speed discretization to observe resonances occurring at variable speed as shown in [2]. Analytical models are usually preferred for early optimization purposes [3].

An analytical approach based on a lumped parameters model has been developed to compute much faster the open-circuit airgap field distribution due to multilayer and multi-segment interior PM [4]. For a given rotor topology, the different magnetic flux paths are identified by running a Finite Element Analysis (FEA), and then approximated with a Magnetic Equivalent Circuit (MEC), or reluctance network. Stator and rotor cores reluctances are neglected and the rotor bridges are supposed to be fully saturated so that leakage fluxes through bridges are imposed.

However, MEC results in an approximated stepwise rotor magnetomotive force (mmf). Though the different steps values are accurately estimated by the MEC, the discontinuous transition between magnetic poles induces a large error on the magnetic field harmonic content. Moreover, it does not include slotting effect and only gives

insight on the radial component of the magnetic field. This introduces an additional error on the magnetic forces computation once the effect of the tangential field cannot be neglected.

In [5], the tangential component and slotting effect are included using the complex permeance method developed in [6]. For this, the IPM magnetization has to be transformed into an equivalent Surface-mounted PM (SPM) magnetization. Besides, a trapezoidal waveform has been introduced to reduce the estimation errors during the pole transitions.

In any case, a first non-linear FEA has to be run in order to create the MEC. In this paper, a fast and accurate method to compute the open-circuit magnetic field of IPM machines is proposed, including slotting effect and both radial and tangential components. The method derives from the one exposed in [5], except that the magnetization is first computed with a non-linear FEA. Furthermore, rotor motion, slotting effect and tangential field are included using the semi-analytical Subdomain Model (SDM) of an equivalent SPM machine [7]. This enables to compute the airgap flux density very quickly and accurately for a large number of time steps [8].

The method is then integrated in MANATEE software [9] for the electromagnetic and vibroacoustic study of the Toyota Prius 2004's IPM machine in open-circuit and with a partial load. The results for the electromagnetic forces are favorably compared with [10] based on fully numerical methods. The vibroacoustic study is based on analytical models presented in [2] and enables to compute the emitted noise and vibrations at variable-speed.

II. THE NEW HYBRID METHOD DESCRIPTION

A. *Introduction*

In this first part, the new hybrid method is developped and compared with the analytical approach of [5], using the IPM machine topology shown on Figure 1. This is the V-shape IPM machine used for the Toyota Prius 2004 with 48 stator slots ($Z_s = 48$) and 8 poles ($p = 4$).

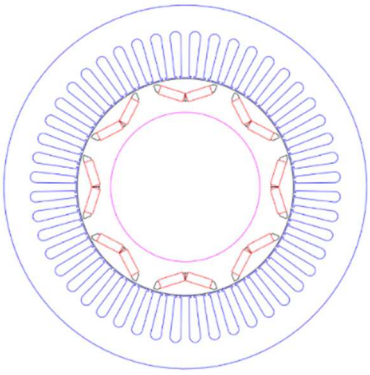

Figure 1 Toyota Prius 2004 IPMSM (48s8p)

B. *Rotor Magnetization Computation*

The rotor magnetization pattern is first computed by a non-linear FEA using FEMM software [11] and without stator slots, as shown in Figure 2. Figure 3 shows the basic MEC which can be established from the FEA flux density plot, where:

- ϕ_r is the magnet remanent flux;
- R_m is the reluctance seen by the magnet leakage flux;
- R_a is the reluctance seen by the magnet end-leakage flux;
- ϕ_{ir} is the leakage flux through the saturated iron bridge;
- R_g is the reluctance seen by the airgap flux.

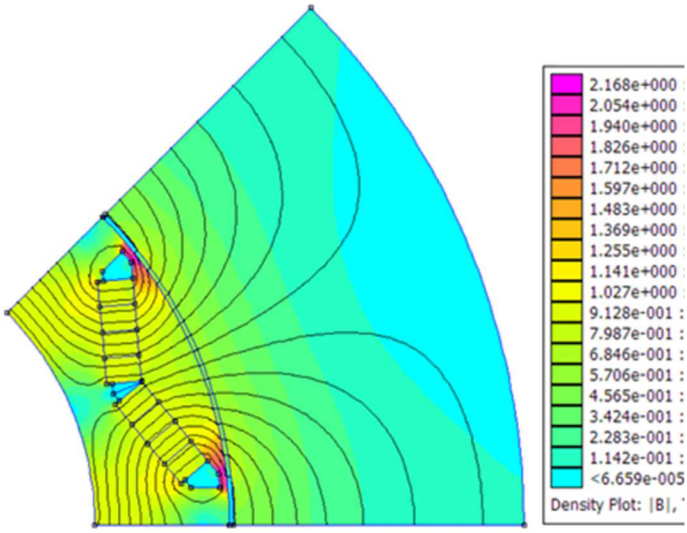

Figure 2 FEMM model of a rotor pole automatically built by MANATEE [7]

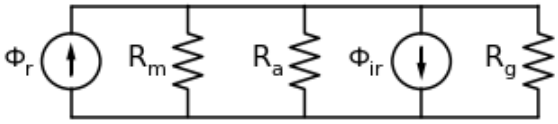

Figure 3 MEC of the rotor pole

Reluctances are computed using the geometrical parameters of the machine. The magnets' remanent flux is imposed by the permanent magnet technology. The leakage flux through the iron bridges is a design parameter depending on the desired saturation level in these bridges according to the $B(H)$ curve of the rotor lamination (see Figure 4). MEC methodology is explained more in details in [3] and [4].

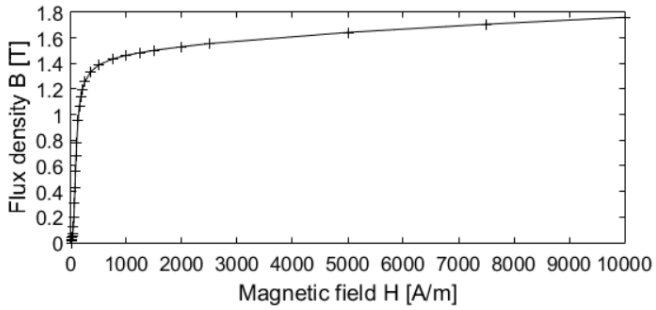

Figure 4 B(H) curve of the laminated steel M400-50A

The different resulting magnetization patterns are shown on Figure 5 for a single pole, where:

- blue line is the magnetization obtained with the non-linear FEA;
- red line is the one obtained with MEC using a stepwise transition between two magnetic poles.
- green line is the one obtained with MEC using a trapezoidal transition.

In conclusion, it is more interesting to directly compute the rotor mmf thanks to a non-linear FEA and use it within an equivalent subdomain model for better accuracy.

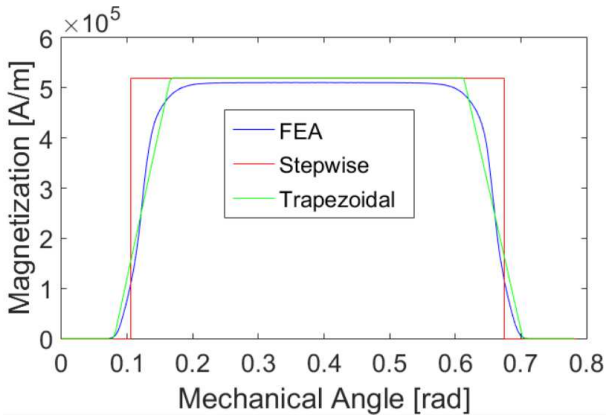

Figure 5 Magnetization patterns comparison between FEA and analytical approach

C. *Equivalent SM Subdomain Model*

The subdomain technique enables to compute both radial and tangential fields in the air gap including stator slotting effect. The magnetic field is obtained for each rotor position by translating the rotor mmf at the mechanical speed. The field equations are developed in [7].

In the present method, the particular solution in the magnets is given by the Fourier series of the magnetization pattern obtained with non-linear FEA (Figure 5). The equivalent SPM is illustrated on Figure 6 with the corresponding MEC. The equivalent SPM remanent flux density is computed using the flux conservation in the air gap:

$$\phi_{spm} = \phi_g \left(1 + \frac{R_g}{R_{spm}}\right) \quad \text{[Wb]} \qquad (1)$$

where:

- ϕ_{spm} is the surface magnet remanent flux;
- R_{spm} is the reluctance seen by the magnet leakage flux;
- R_g is the reluctance seen by the air gap flux computed in the previous paragraph.

The magnet length is arbitrarily set as very small compared with the airgap length.

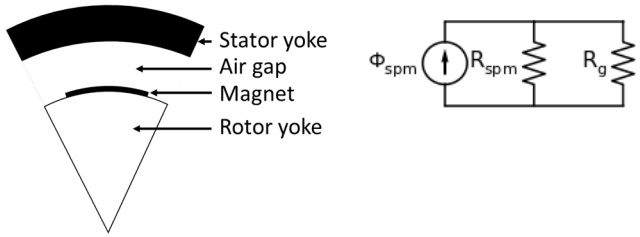

Figure 6 Equivalent SPM rotor and MEC

The resulting radial and tangential flux densities are shown on Figure 7 and Figure 8 at the initial rotor position, in comparison with a non-linear FEA including slots. Results are in good agreement with FEA, hence the method is validated for the flux density computation. The overall calculation time on a standard laptop is 5 *s* to obtain the full airgap field in both directions with 2048 time steps over a mechanical period and 2048 angular steps along the airgap.

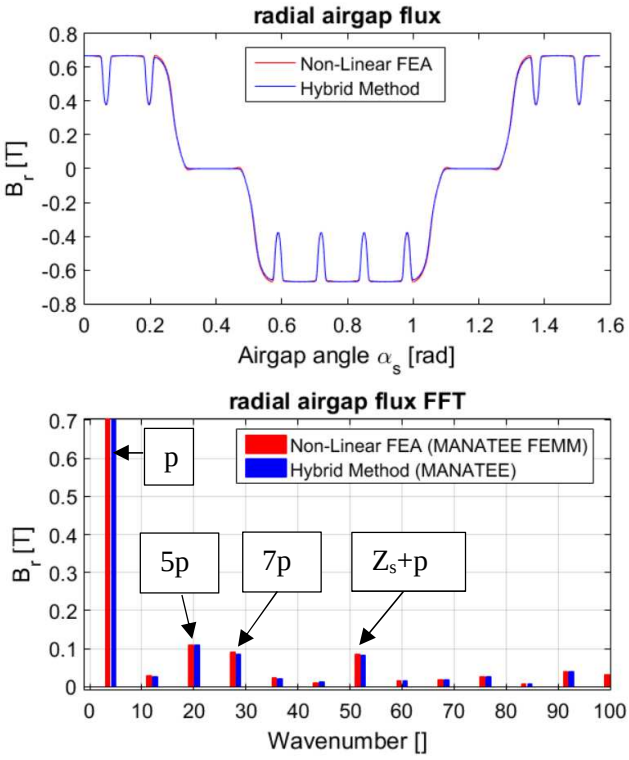

Figure 7 Radial flux density and spatial FFT at open-circuit

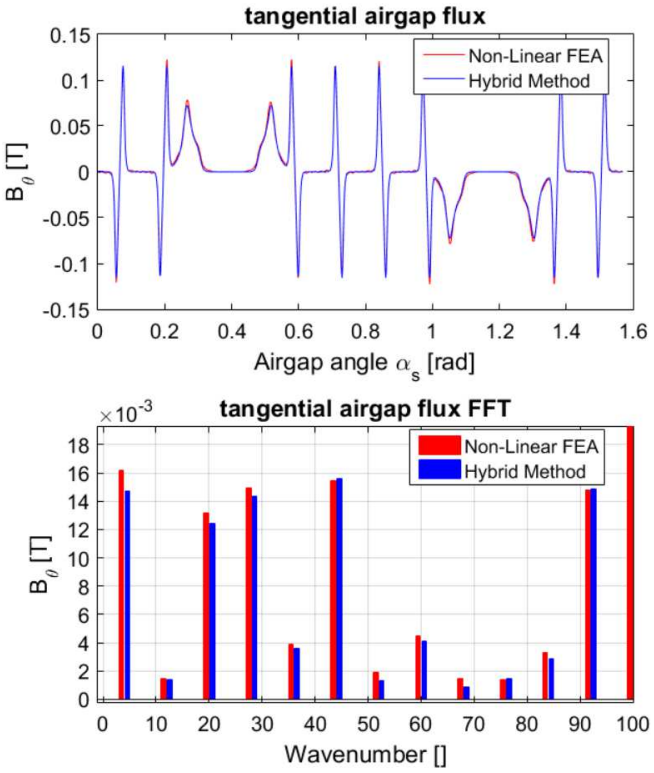

Figure 8 Tangential flux density and spatial FFT

III. VIBROACOUSTIC MODELS

A. *MANATEE Simulation Software*

MANATEE is a multiphysics simulation environment dedicated to the fast prediction of noise and vibrations at variable speed of electrical machines for design purpose. The simulation process relies on several linked modules accounting for the electric, electromagnetic, mechanical and acoustic behavior of the machine, as shown on Figure 9. Each model can be either analytical or numerical (FEA) for a better compromise between computation time and accuracy. MANATEE's principles are explained more in details in [2].

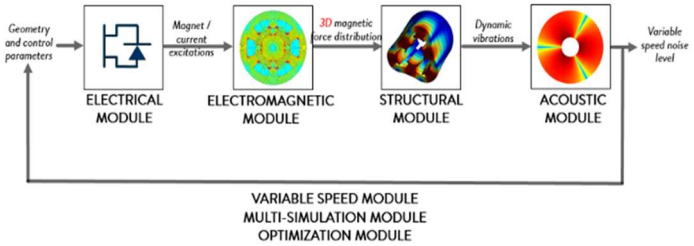

Figure 9 Multiphysics models included in MANATEE

B. *Electromagnetic Module*

In this study, the magnetic flux density is computed with the hybrid method presented in the previous section. Radial and tangential magnetic pressures are then deduced by computing the Maxwell stress tensor at the middle of the air gap, such as:

$$P_{rad}(t,\theta) = \frac{B_{rad}^2(t,\theta) - B_{tan}^2(t,\theta)}{2\mu_0} \; [N.m^{-2}] \quad (2)$$

$$P_{tan}(t,\theta) = \frac{B_{rad}(t,\theta)B_{tan}(t,\theta)}{\mu_0} \quad [N.m^{-2}] \quad (3)$$

with $B_{rad}(t,\theta)$ and $B_{tan}(t,\theta)$ the radial and tangential flux density computed in the previous part. Equation (2) shows that the tangential flux densities impacts the radial forces even if the magnitude of the fundamental tangential flux density is lower than the one of the radial flux density. It is not necessarily the case for higher spatial harmonics hence the tangential flux density should not be neglected even if this assumption is correct for specific cases [12].

Furthermore, it is commonly assumed that the radial pressure is only responsible for the radial vibrations of the stator yoke that generate noise. This assumption is made in the next study under MANATEE because radial pulsating magnetic forces (wavenumber $r = 0$) are responsible for audible magnetic noise on this particular machine. However, a tangential force harmonic of wavenumber $r >= 2$ may induce a radial deflection of the stator yoke through bending of the stator teeth [13].

C. *Vibroacoustic Module*

The chosen mechanical module is analytical, based on modal superposition using Frequency Response Functions (FRF). The equations used for this particular model can be found in [14]. The principle is to compute the total vibration level by summing all the contribution of each harmonic of pressure regarding the stator's structural modes and their natural frequency. Each contribution is computed separately by modeling the stator structure as an equivalent ring. More advanced structural models including the tooth bending motion using a coupling with finite element software GetDP or OptiStruct are available in MANATEE but the paper objective is to illustrate how the new electromagnetic method can be used for fast vibroacoustic design of electric machines.

Harmonics of Maxwell radial pressure are obtained by performing a 2D Fourier series of the spatio-temporal pressure distribution:

$$P_{rad}(t,\theta) = \sum_{f,r} P_{fr} e^{j(2\pi f t - r\theta + \varphi_{fr})} \quad (4)$$

where:

- (f,r) is the couple of frequency and wavenumber for each pressure harmonic;
- P_{fr} is the magnitude of the harmonic (f,r);
- φ_{fr} is the phase of the harmonic (f,r);

The natural frequency f_m of each stator structural mode m is obtained with analytical formulas given in [14]. The vibration level is strongly amplified when a harmonic of pressure excites and resonates with a structural mode. Such resonance occurs when the excitation's wavenumber is the same as the mode's order and the excitation's frequency is close to the natural frequency of the mode, meaning:

$$\begin{cases} r = m \\ f \approx f_m \end{cases} \quad (5)$$

Pulsating pressure harmonics with $r = 0$ may excite the 0^{th} structural mode, commonly named "breathing mode". Pressure harmonics with wavenumber $r = 1$ induce an unbalanced magnetic pull (UMP) which can excite a rotor bending mode, not accounted here in 2D. Finally, any pressure harmonics whose wavenumber is greater than $r = 2$ ("rotating" harmonics) can generate vibrations in the stator structure and potential noise.

In PM machines, it is shown that the least non-zero wavenumber r_{min} is given by the rule:

$$r_{min} = GCD(Z_s, 2p) \quad (6)$$

The least non-zero frequency f_{min} for the 0^{th} wavenumber at open-circuit is given by the second rule:

$$f_{min} = LCM(Z_s, 2p)\frac{f_0}{p} \quad (7)$$

where $f_0 = pN/60$ is the electric synchronous frequency, with N the rotor mechanical speed in Revolution Per Minutes (RPM).

D. Acoustic Module

The chosen acoustic model analytically computes the sound pressure and power levels from the stator structure level of vibrations. It is based on the radiation efficiency model developed in [15]. The lowest orders of structural modes generally have a higher radiation efficiency and the 0^{th} order must be particularly taken care of for traction application [10][16].

IV. Vibroacoustic Results For Prius IPM

A. Open-circuit electromagnetic results and validation

MANATEE results are compared with the results presented in [10] for the study of electromagnetic forces in the Prius' IPM at open-circuit. The radial flux density waveform at open-circuit shown on Figure 4)a in [10] is very close to the one computed with the new hybrid method presented in this article. The radial pressure FFT2 shown on Figure 10 is also in good agreement with Figure 10)a of [10].

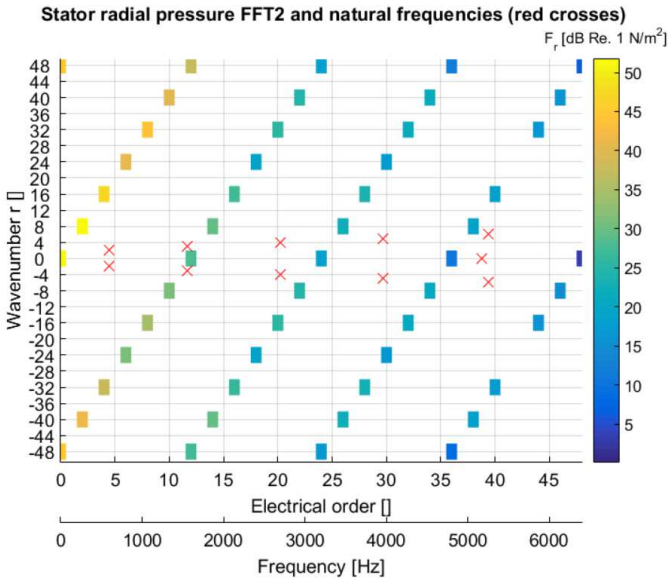

Figure 10 Radial pressure FFT2 at open-circuit, N=2000 RPM

Every harmonic of pressure has a wavenumber multiple of 8, which is indeed the lowest wavenumber $r_{min} = 8$ predicted by Equation (6). The first frequency of pulsating radial pressure ($r = 0$) at open-circuit is at $f = 12f_0$, as given by Equation (7). When the rotation speed N increases, every harmonic of pressure is translated towards the right of the figure. In conclusion, the magnetic pressure may only excite stator lamination structural modes of orders $m = 0, 8, 16$ etc. The topology of the Prius IPM prevents from exciting low structural modes except the 0^{th}-order. The frequency of the main pulsating pressure at $f = 12f_0$ is quite low and so it will excite the breathing mode at high speeds [10]. However, higher harmonics of pulsating pressure may resonate with the mode 0 at lower speeds.

B. Open-circuit vibroacoustic results and validation

The natural frequencies of the machine have been calculated in [10] using both FEA and analytical models and assuming free boundary conditions. The comparison with MANATEE's analytical structural model is shown in . As said in the previous part, only the structural modes of order $m = 0, 8$ are problematic.

	$m = 0$	$m = 2$	$m = 3$	$m = 4$
MANATEE	5173 Hz	591 Hz	1548 Hz	2702 Hz
FEA [10]	X	617 Hz	1620 Hz	2772 Hz

Table 1 Structural modes and associated natural frequency comparison between MANATEE's analytical model and FEA [9]

The vibroacoustic simulation of the Prius' IPM is made under open-circuit condition at variable speed between 500 and $7000\ RPM$, for a total computation time around 6 seconds for 200 speed steps. In fact, most of the time is

dedicated to the electromagnetic simulation (5 s). In the model, the microphone is 1 meter away from the machine.

Figure 11 shows the overall emitted sound in dBA at each rotating speed and the contribution of each structural mode. The maximum sound power level is reached at $N = 6450\,RPM$ due to the first pulsating radial pressure which resonates with the breathing mode at $f_n = 5173\,Hz$. The resonance can also be observed on the radial pressure FFT2D (cf. Figure 12). The resonance at $N = 3240\,RPM$ is due to the interaction between the breathing mode and the 2nd pulsating excitation at $f = 24f_0$. The sonagram on Figure 13 shows the evolution of the noise spectrum in function of rotation speed

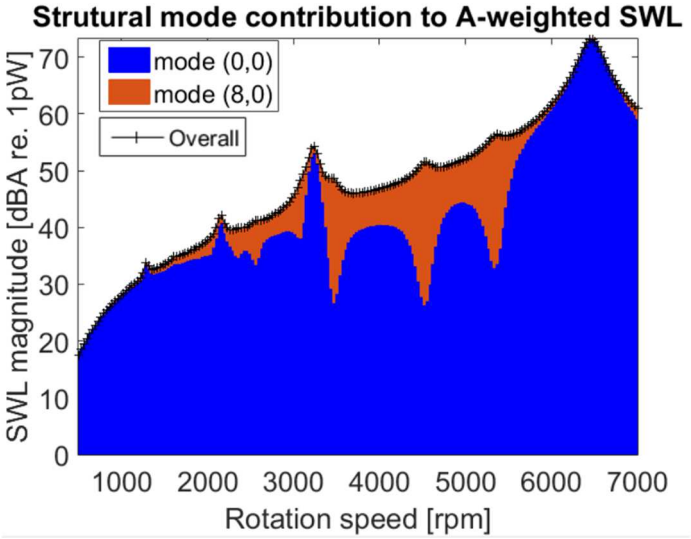

Figure 11 Overall sound power level at variable speed in dBA obtained with MANATEE, including modal contribution

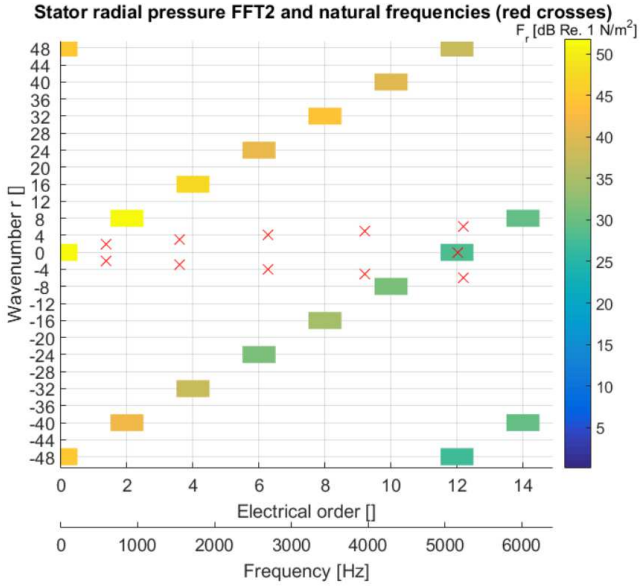

Figure 12 Radial force FFT2 at open-circuit, N=6450 RPM. The first pulsating harmonic resonates with breathing mode at $12f_0$

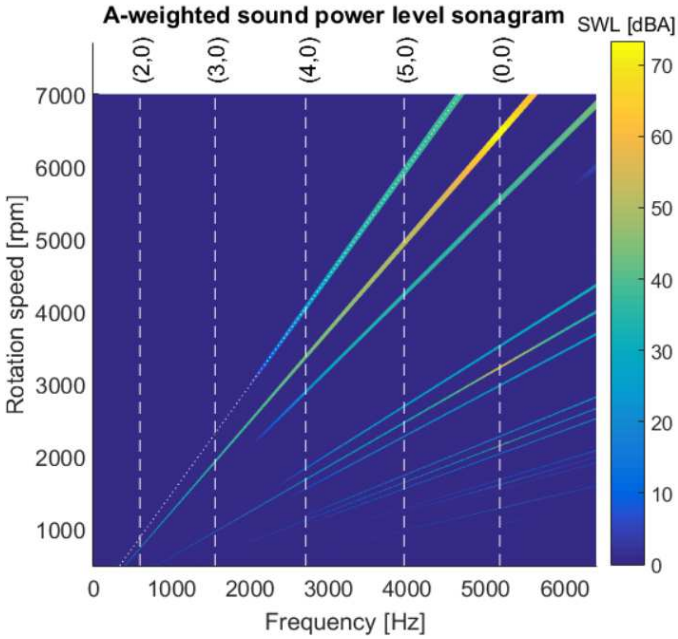

Figure 13 Sonagram of the sound power level [dBA]

One can see that the contribution of the mode m=8 is negligible at open-circuit condition. In fact, the natural frequency of the 8^{th}-order mode is estimated at $7850\,Hz$ and is only excited by very small harmonics of pressure under $7000\,RPM$.

C. *Extension to partial load*

Assuming that the airgap field is the sum of the armature and magnet fields, the hybrid method based on SDM can be used to calculate the radial and tangential field created by the stator distributed winding, as in [7]. This implies that the stator saturation is neglected and the rotor saturation is the same as in open-circuit. However, such simulation enables to check if the winding harmonics do not create additional magnetic forces and strong resonances during variable speed operation.

In this example, a partial load is simulated with null I_d current, $I_q = 10A\,RMS$ and the current angle is equal to 90°. In this case, the machine operates at constant exciting current for the same speed range between 500 and 7000 RPM. The air gap flux density is calculated by both hybrid SDM and non-linear FEA (using MANATEE and FEMM coupling) to see the effect of the armature field and check the new saturation level (see Figure 14). The saturation increases the virtual air gap length (given by Carter's coefficient) and so decreases the fundamental magnitude. Moreover, a new spatial harmonic appears at $r = 3p = 12$ which is the first saturation harmonic. Except these two differences, the flux density spectrum at partial load contains the same non-zero harmonics as in open-circuit.

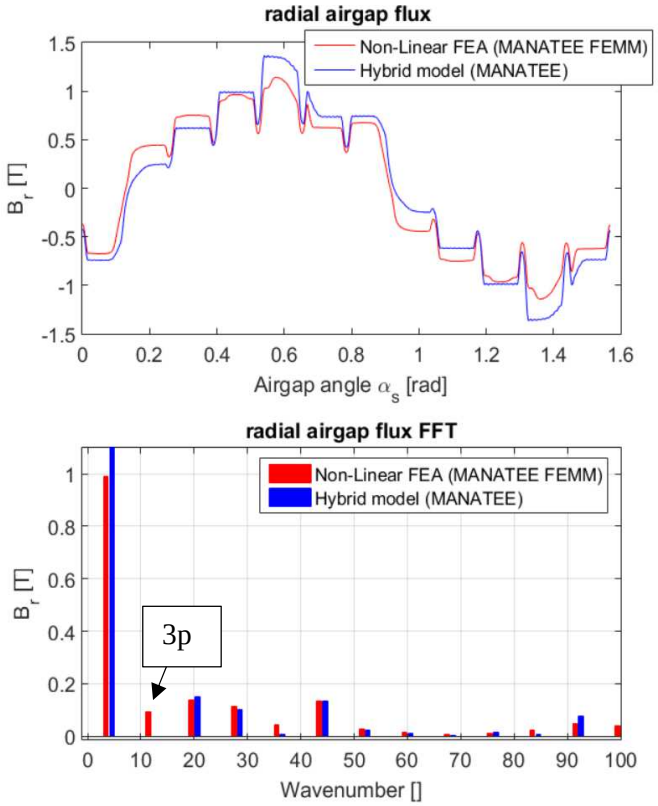

Figure 14 Radial flux density and spatial FFT at partial load

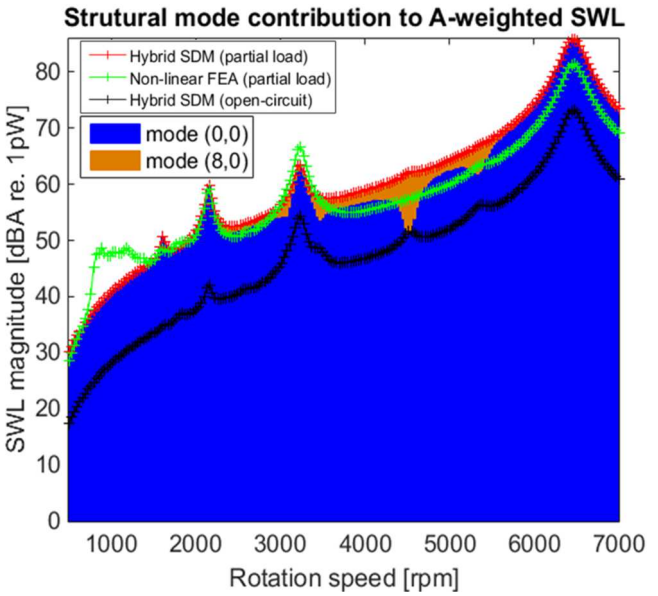

Figure 15 Overall sound power level at variable speed in dBA. Comparison between non-linear FEA and hybrid method at partial load regarding the open-circuit case.

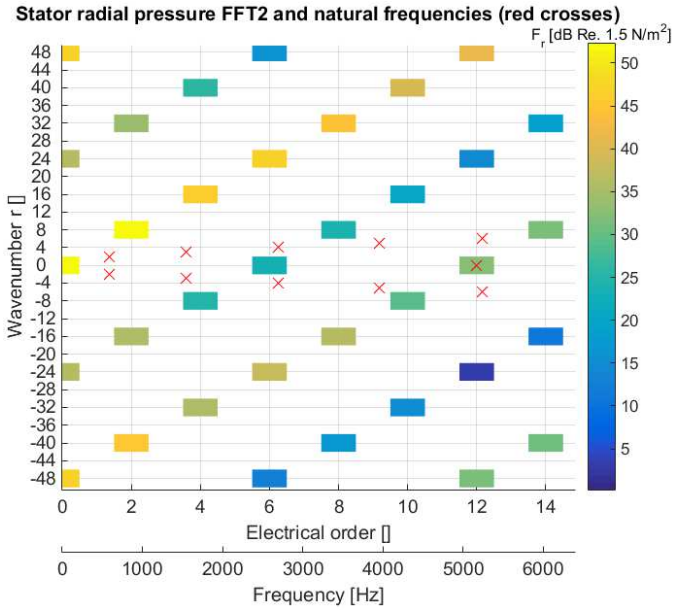

Figure 16 Radial force FFT2 at partial load, N=6450 RPM. The first pulsating harmonic is now at $6f_0$ but the main pulsating harmonic still resonates with breathing mode at $12f_0$

Figure 15 shows the comparison of the variable magnetic noise level at partial load with non-linear FEA and the hybrid method, and in the open-circuit case. Both sonograms at partial load are quite close while the gap is less than 5 dB and resonances are superimposed. Compared with the open-circuit case, no new resonance is observed and noise is even more due to the breathing mode of (m=0) of the stack. These excitations are linked to torque generation. The overall sound power level is higher because the armature field induces additional radial magnetic forces as illustrated on Figure 16. The first pulsating harmonic ($r = 0$) is now at $f = 6f_0$ due to the interaction of the first winding flux density harmonic at frequency $f = f_0$, and wavenumber $r = -5\text{p}$ with the flux density harmonic at frequency $f = 5f_0$ and wavenumber $r = 5\text{p}$. The main resonance with the breathing mode is still due to the largest pulsating harmonic at $12f_0$.

In conclusion, the hybrid model (subdomain model of armature field and subdomain model of magnet field based on FEMM magnetization coefficient) is still valid to calculate main Maxwell resonances at partial load. Besides, the air gap flux density knowledge enables to estimate very quickly torque ripple and electromotive force. Thus, the hybrid model can be used to minimize noise and vibrations due to electromagnetic forces as well as torque ripple, cogging torque and EMF distortion thanks to the knowledge of the air gap flux density.

V. CONCLUSION

A new hybrid method has been proposed for the accurate and fast prediction of air gap magnetic field in open-circuit and partial loaded IPM machines. The rotor non-linearity and geometrical complexity are taken into account with a single non-linear FEA simulation which enables to define the magnetization of an equivalent surface magnet and compute the field for any rotor position by means of the subdomain method initially developed for SPMSM. This hybrid method enables optimization and topology exploration, especially including variable speed vibroacoustic study, within a few seconds for one topology.

Applying this modeling technique in MANATEE software for the evaluation of noise and vibrations due to magnetic forces, it is shown that the maximum noise and vibration levels at open-circuit are due to the pulsating radial pressure which resonates with the breathing mode at high speed on Toyota Prius 2004. The multiphysics simulation takes 6 seconds and lead to same conclusions as the full FEA method exposed in [10] which takes several hours of simulation.

In further studies, noise and torque ripple reduction techniques available in MANATEE software such as skewing, magnet shaping, stator notches and wedges, and current injection will be applied.

REFERENCES

[1] M. Valavi, A. Nysveen, R. Nilssen, R. D. Lorenz, and T. Rølvåg, "Influence of pole and slot combinations on magnetic forces and vibration in low-speed PM wind generators," *IEEE Trans. Magn.*, vol. 50, no. 5, pp. 1–11, 2014.

[2] J. Le Besnerais, "Fast Prediction of Variable-Speed Acoustic Noise and Vibrations due to Magnetic Forces in Electrical Machines," in *ICEM International Conference on Electrical Machines*, 2016.

[3] H. Mirahki, M. Moallem, and S. A. Rahimi, "Design optimization of IPMSM for 42 v integrated starter alternator using lumped parameter model and genetic algorithms," *IEEE Trans. Magn.*, vol. 50, no. 3, pp. 114–119, 2014.

[4] L. Zhu, S. Z. Jiang, Z. Q. Zhu, and C. C. Chan, "Analytical Modeling of Open-Circuit Air-Gap Field Distributions in Multisegment and Multilayer Interior Permanent-Magnet Machines," *IEEE Trans. Magn.*, vol. 45, no. 8, pp. 3121–3130, 2009.

[5] H. Mirahki and M. Moallem, "Analytical Prediction of Cogging Torque for Interior Permanent Magnet Synchronous Machines," *Prog. Electromagn. Res.*, vol. 37, no. April, pp. 31–40, 2014.

[6] D. Žarko, D. Ban, and T. A. Lipo, "Analytical calculation of magnetic field distribution in the slotted air gap of a surface permanent-magnet motor using complex relative air-gap permeance," *IEEE Trans. Magn.*, vol. 42, no. 7, pp. 1828–1837, 2006.

[7] T. Lubin, S. Mezani, and A. Rezzoug, "2-D exact analytical model for surface-mounted permanent-magnet motors with semi-closed slots," *IEEE Trans. Magn.*, vol. 47, no. part 2, pp. 479–492, 2011.

[8] E. Devillers, J. Le Besnerais, T. Lubin, M. Hecquet, and J. P. Lecointe, "A review of subdomain modeling techniques in electrical machines : performances and applications," in *ICEM International Conference on Electrical Machines*, 2016.

[9] Eomys Engineering, "MANATEE," 2016. [Online]. Available: http://eomys.com/produits/manatee.

[10] Z. Yang, M. Krishnamurthy, and I. P. Brown, "Electromagnetic and vibrational characteristic of IPM over full torque-speed range," *Proc. 2013 IEEE Int. Electr. Mach. Drives Conf. IEMDC 2013*, pp. 295–302, 2013.

[11] D. Meeker, "Femm." [Online]. Available: http://www.femm.info.

[12] Z. Q. Zhu, Z. P. Xia, L. J. Wu, and G. W. Jewell, "Analytical modeling and finite-element computation of radial vibration force in fractional-slot permanent-magnet brushless machines," *IEEE Trans. Ind. Appl.*, vol. 46, no. 5, pp. 1908–1918, 2010.

[13] H. Lan, J. Zou, Y. Xu, M. Liu, and B. Zhao, "Vibration induced by radial and tangential force harmonics in permanent magnet synchronous machines," *IEEE Trans. Magn.*, vol. (To be pub, 2017.

[14] J. Le Besnerais, V. Lanfranchi, M. Hecquet, P. Brochet, and G. Friedrich, "Prediction of audible magnetic noise radiated by adjustable-speed drive induction machines," *IEEE Trans. Ind. Appl.*, vol. 46, no. 4, pp. 1367–1373, 2010.

[15] P. L. Timar, *Noise and vibration of electrical machines*. Elsever, 1989.

[16] A. Hofmann, F. Qi, T. Lange, and R. W. De Doncker, "The breathing mode-shape 0: Is it the main acoustic issue in the PMSMs of today's electric vehicles?," *2014 17th Int. Conf. Electr. Mach. Syst. ICEMS 2014*, pp. 3067–3073, 2015.